Article **Journal of Chemical and Physical Energy**
June 2023, Vol.10 No.28 8-15

Removal of disperse blue textile dye 56 from water using a metal-organic framework of erbium

Eliminación del colorante textil azul disperso 56 del agua utilizando una estructura metalorgánica de erbio

MORA-VARGAS, Etnia Valeria† & LOERA-SERNA, Sandra*

Universidad Autónoma Metropolitana, Unidad Azcapotzalco

ID 1st Author: *Etnia Valeria, Mora-Vargas* / **ORC ID**: 0009-0004-3348-3587, **CVU CONAHCYT ID**: 1267599

ID 1st Co-author: *Sandra, Loera-Serna* / **ORC ID**: 0000-0001-9562-3195, **CVU CONAHCYT ID**: 172467

DOI: 10.35429/JCPE.2023.28.10.8.15 Received March 15, 2023; Accepted June 30, 2023

Abstract

The disperse blue dye 56 (AD56) is of the anthraquinone type and is considered an important source of water pollution due to the discharges generated by the textile industry. An efficient way to eliminate it is using porous materials, for example, metal-organic networks (MOF). In this work, the adsorption of AD56 with an Er MOF was studied and synthesized by microwave-assisted method and using 1,4-benzene dicarboxylic acid (BDC) as an organic ligand. Physicochemical analysis of the Er_2BDC_3 was carried out by XRD, FTIR, SEM, and UV-Vis spectroscopy to determine the dye concentration. Due to its high porosity, the results show that the MOF can be reused for up to seven adsorption cycles for the AD56 dye. The adsorption process changed the structure of the MOF, obtaining a more pure and stable material in an aqueous medium. The maximum AD56 adsorption capacity obtained was 33.97 mg/g after seven cycles. This material can be used in consecutive adsorption processes and for other anthraquinone dyes.

Metal-organic frameworks, Dyes, Adsorption

Resumen

El colorante azul disperso 56 (AD56) es de tipo antraquinónico y se considera una fuente de contaminación de agua importante debido a las descargas que genera la industria textil. Una forma eficiente de eliminarlo es mediante el uso de materiales porosos, por ejemplo, las redes metal-orgánicas (MOF). En este trabajo se estudió la adsorción de AD56 con una MOF de Er, sintetizada mediante microondas y empleando el ácido 1,4- bencenodicarboxílico (BDC) como ligante orgánico. El análisis fisicoquímico de la Er_2BDC_3 se llevó a cabo mediante DRX, FTIR, SEM y se utilizó espectroscopia UV-Vis para determinar la concentración de colorante. Los resultados muestran que la MOF puede ser reutilizada hasta siete ciclos de adsorción para el colorante AD56, esto debido a la alta porosidad. El proceso de adsorción cambió la estructura de la MOF, obteniéndose un material con mayor pureza y estable en medio acuoso. La máxima capacidad de adsorción de AD56 obtenida fue de 33.97 mg/g después de siete ciclos. Este material puede utilizarse en proceso de adsorción consecutivos y para otros colorantes antraquinónicos.

Redes metal orgánicas, Colorantes, Adsorción

Citation: MORA-VARGAS, Etnia Valeria & LOERA-SERNA, Sandra. Removal of disperse blue textile dye 56 from water using a metal-organic framework of erbium Journal of Chemical and Physical Energy. 2023. 10-28: 8-15

* Correspondence to the Author (e-mail: sls@azc.uam.mx)
† Researcher contributing as first author.

Introduction

The generation of textile dyes, given the industrial demand, was affected due to the insufficiency of materials of natural origin; This resulted in the creation and production of synthetic dyes with the same characteristics as the natural ones. The most widely used industrial dyes are anthraquinones due to their high resistance to biodegradation, sun exposure, and chemical attack. (Martínez, *et al.,* 2014) Small amounts of these materials can color large quantities of water; they also greatly damage flora, fauna, and human life due to their toxic, mutagenic, and carcinogenic effects. (Doval, 2014) Around 10,000 dyes are used in various industrial processes.

It is estimated that from 2 to 50% are discarded in wastewater and considered pollutants that cannot be removed by conventional methods in water treatment. Removing these dyes has been an environmental problem, which has encouraged the development of new technologies and methods for their removal and thus reducing their environmental impact. (Piñón, 2019; Núñez & Victoria, 2020)

One way to remove colorants from water is by using porous materials, among which are metal-organic frameworks (MOFs). MOFs are coordination polymers of metal ions with organic ligands forming one-, two- or three-dimensional crystal lattices. (Sorribas & Téllez, 2016; Loera-Serna, *et al.,* 2019). The union of these two units gives rise to different types of coordination, which depend on the symmetry of the linker and the coordination number of the metal center. (Loera-Serna, *et al.*, 2012).

Its characteristics include high structural and composition versatility, different pore sizes, high specific surfaces, pore volumes, exposed metal centers, and structural flexibility. (Rodríguez, 2019) Among the great variety of MOFs, the LnMOFs (lanthanide metal-organic networks) can be found, which present characteristics such as ionic radii variation, high selectivity, and highly porous structures. In a 2017 study, an erbium MOF (Er-MOF) was used for the adsorption of methylene blue from an aqueous solution, achieving a maximum removal capacity of 92%. The MOF was synthesized hydrothermal and characterized by FT-IR, XRD, and SEM.

The material presented high stability in water and an accessible nanometric opening, which could make it a good adsorption material for polluting effluent dyes. The adsorption, thermodynamic and kinetic isotherm resulted in a porous material that conforms to the Langmuir isotherm. In addition, the adsorption process took about 30 minutes, and it is a process with low cost and high adsorption efficiency. (Mohammadnejad *et al.,* 2018)

This work synthesized an erbium-based organic metal-type adsorbent material to remove the disperse blue anthraquinone dye 56 from water. The study of the physicochemical properties of the material was carried out using X-Ray diffraction (XRD), Fourier transform infrared spectroscopy (FT-IR), and scanning electron microscopy (SEM). The adsorption capacity was determined by ultraviolet-visible spectroscopy (UV-Vis), and due to the high adsorption capacity of the MOF, several adsorption cycles were performed for the analyzed dye.

Methodology

MOF synthesis

The synthesis was carried out using 1.5 mmol of the organic ligand BDC, which was dissolved in 30 mL of N, N-dimethylformamide (DMF), and 1 mL of methanol with 0.1 g of $NaHCO_3$ was added; this solution was stirred. On the other hand, 0.5 mmol of de $ErCl_3 \cdot H_2O$ was dissolved in 3 mL of methanol; this second solution was added drop by drop to the first solution with DMF and stirred at a T=50°C for 8 hours. At the end of agitation, the mixture was placed in glass vials of 30 mL each, and The Anton Paar was used with a heating ramp of 5 minutes until reaching T=150°C. It was kept like this for 15 minutes, then the temperature dropped to T=55°C. The powders obtained were washed with methanol in a centrifuge at 12,000 RPM.

Dye adsorption

A solution was prepared with 100 mL of deionized water with a known concentration of disperse blue anthraquinone dye 56. For the calibration curve, solutions were synthesized, and with a UV-Vis spectrophotometer, maximum absorbance data were obtained for the different concentrations.

ISSN: 2410-3934

Finally, a wavelength of 545 nm was obtained for maximum absorbance. Adsorption was performed by adding 0.2 g of the MOF in 10 mL of the stock solution. To determine the amount of dye adsorbed by the MOF, NanoDrop brand UV-Vis spectroscopy was used, and the calibration curve was performed with a maximum concentration of 100 ppm.

Characterization of the MOF

The XDR of the MOF before and after adsorption was performed in a Philips X'PERT PRO equipment with a monochromator with copper anode (45 Kv and 40 mA), with a scanning speed of 0.11% and a range of 2θ from 5 to 50°C. This technique was used to determine the formation of the MOF by comparing the diffractogram with the CCDC database (Kennard *et al.*, 1965). To obtain the spectroscopy with Fourier transform (FT-IR), Bruker Tensor-27 equipment was used, with a spectral range of 4000-400 cm^{-1} at room temperature, using the attenuated total reflection (ATR) technique with a resolution of 2 cm^{-1} and 24 scans. The morphology of the MOF was determined by scanning electron microscopy using a ZEIZZ supra 55VP instrument coupled with a 2kV voltage elemental analysis probe without sample coating.

Results

Physicochemical properties of the MOF

Figure 1 represents the experimental diffractogram obtained for pristine MOF and compared with the simulated ones for Tb_2BDC_3 reported by Reineke *et al.* (1999), which is registered in the CCDC database as QACTUJ and Er_2BDC_3 reported by Chen *et al.*, (2006) both were obtained from the microwave-assisted solvothermal method.

It can be observed that the experimentally obtained pattern represents characteristic peaks of high and low intensity at different Bragg angles, which match those reported for Tb_2BDC_3 represented with an (**x**) and Er_2BDC_3 represented with an (+). The structure obtained for MOF-Er is not reported in theory, the comparison can be made with the simulated XRD pattern of terbium and erbium MOF structures.

Due to obtaining various crystalline compounds, the percentage of each structure present in the MOF-Er was calculated using the following equations:

For the total intensity:

$$I_T = \sum I_x + \sum I_+ + \sum I_F \quad (1)$$

Where the total intensity (I_T) is equal to the sum of the intensity of terbium (I_X), erbium (I_+) and funds (I_F).

For the percentage of crystalline phase:

$$\%\ phase = \frac{\sum I_{(x,+)}}{\sum I_T}(100)$$

Table 1 shows a higher percentage of the Er_2BDC_3 structure reported by Chen *et al.* (2006).

Material	% crystalline phase
Tb_2BDC_3	25.46
Er_2BDC_3	56.85
Funds	20.70

Table 1 Percentage of crystalline phases in MOF

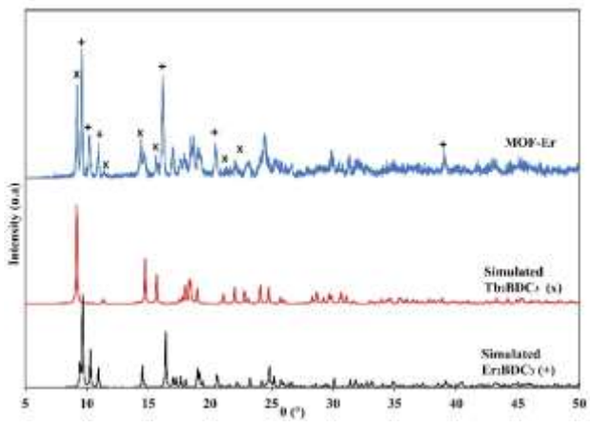

Figure 1 Diffractogram of Er_2BDC_3 synthesized by microwave-assisted method compared to Tb_2BDC_3 and Er_2BDC_3

The crystal size of the MOF-Er sample was determined using the Debye-Scherrer equation:

$$D = \frac{K\lambda}{BCos\theta} \quad (2)$$

Where: D is the crystal size, K is Scherrer's constant, λ is the wavelength in Å, B is the width of peak at half-height in radians, and θ is the peak angle in radians.

ISSN: 2410-3934

Two characteristic peaks were taken in the MOF-Er, each corresponding to Tb_2BDC_3 and Er_2BDC_3. Table 2 shows the values obtained for the crystal size for these two peaks. It is observed that the largest size corresponds to the structure Tb_2BDC_3; this could be attributed to the fact that there is greater compaction in the network parameter of that structure and by the Van der Waals interactions that are generated in the material, which causes more remarkable growth of the crystals.

2θ	D (nm)
9.22 (Tb_2BDC_3)	56.92
16.17 (Er_2BDC_3)	41.15

Table 2 Crystal size for the Er_2BDC_3

Morphology

Figure 2 shows the micrographs obtained magnifications for Er_2BDC_3. Figure 2a shows a microstructure in the form of a rectangular prism at 25,000 magnifications; this structure has sizes of 11.6 μm in height, side a =3.6 μm and side b =4.6 μm, also the bottom you can see an aggregate (red circle) with an asymmetrical shape that has a length of 6.26 μm and width of 2.53 μm Figure 2b. An approximation of 50,000 magnifications of the structure observed in Figure 2a was made. The porosity of the material can be readily appreciated with grains of 0.30-1.0 μm.

Figure 2c) shows structures with a shape corresponding to a rhomboid prim with a larger diagonal D =17.25 μm and smaller diagonal d = 9.75 μm. Finally, Figure 2d at 10,000 magnifications shows that Er_2BDC_3 comprises microstructures of different sizes and asymmetrical shapes with grains sizes from 0.30-1.5 μm. On the surfaces of the microstructures, it is easy to see holes called *pores*, which can be related to the interaction and nature of the reagents used in synthesizing the material.

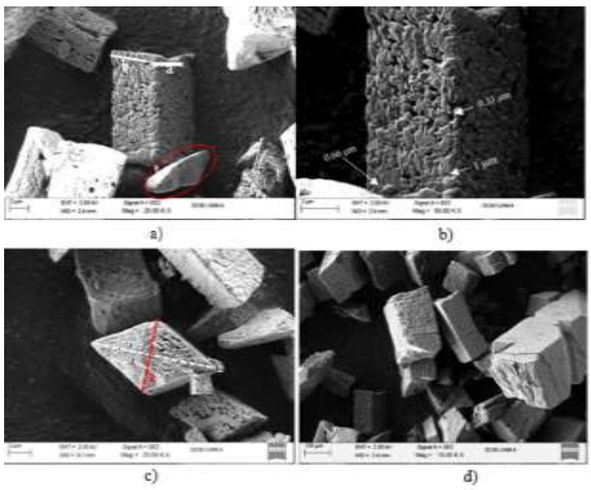

Figure 2 Micrographs of Er_2BDC_3 at a different magnification; a) 25,000, b) 50,000, c) 20,000, and d) 10,000

Functional groups Er_2BDC_3

Figure 3 shows the FT-IR of Er_2BDC_3 synthesized by a microwave-assisted solvothermal method using DMF as an organic solvent and terephthalic acid (BDC) as an organic ligand. The bending vibration of the O-H bond of the carboxylic group (COOH) is observed at 835 cm^{-1} (Wang et al., 2016). The bands in the 1394-1573 cm^{-1} range correspond to the C-C stretching vibration of the 1,4-disubstituted mononuclear aromatic ring structure (Larkin, 2018).

The band of the metal-oxygen bonds is also observed in a range of 400-560 cm^{-1} (Liu *et al.*, 2009), belonging to the Er-O bond. Finally, bands can be observed at 677, 1159, 1255, and 1676 cm^{-1} (Saito *et al.*, AIST), characteristic of the DMF. However, not all the characteristic bands of this compound appear; it is observed that an amount was not removed by washing and is still present in Er_2BDC_3.

The result is expected due to the electron-donating nature of DMF, which coordinates with the Lewis acid sites generated by the erbium coordination deficiency of the hybrid lattice.

ISSN: 2410-3934

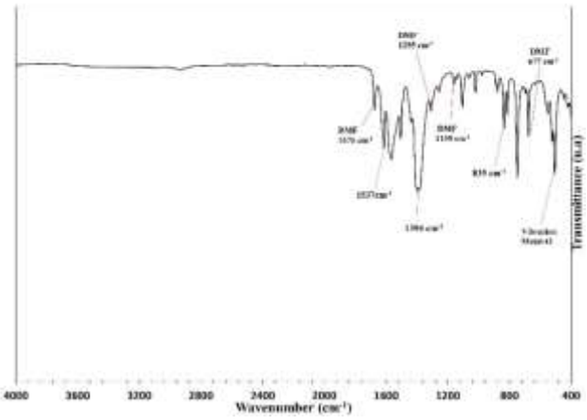

Figure 3 FT-IR spectrum for Er_2BDC_3 synthesized with DMF as an organic solvent

Dye adsorption

Calibration curve for dye AD56

For the construction of the calibration curve, a stock solution was prepared with an initial concentration of C_0 = 100 ppm of the anthraquinone dye AD56. Subsequently, solutions of 90 to 10 ppm were prepared, and for the absorbance measurements of the different concentrations, UV-Vis spectroscopy was used to obtain the spectrum shown in Figure 4.

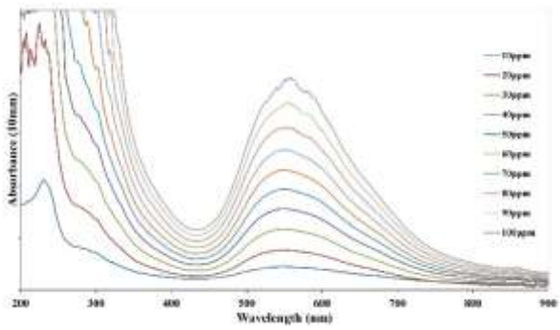

Figure 4 UV-Vis spectrum of disperse blue 56 at different concentrations

Figure 4 shows that the absorbance is directly proportional to concentration. A wavelength λ = 545 nm was chosen for the calibration curve, and the maximum absorbance was obtained for each concentration.

The corresponding linear adjustment was made to obtain an equation of the form:

$$C[ppm] = m(abs) + b$$

Where C is the unknown concentration in the solution in ppm, m is the slope of the line, Abs is the maximum absorbance at time t, and b is the ordinate to the origin.

A correlation factor R^2 =0.9995 was obtained; this indicated that the wavelength selected for the maximum absorbance is adequate. Figure 5 shows the calibration curve obtained for the anthraquinone dye studied.

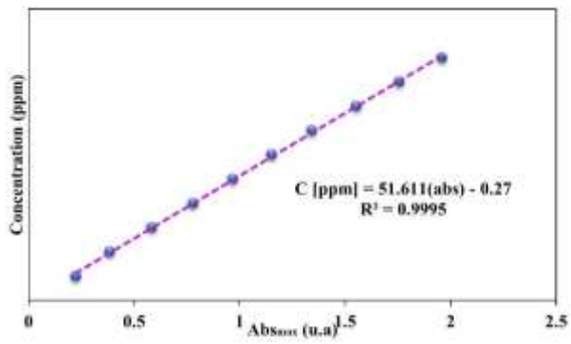

Figure 5 Calibration curve for disperse blue 56

Adsorption cycles

Adsorption was performed by adding 0.2 g of Er_2BDC_3 to 10 mL of 100 mg/g of dye solution. This mixture was left stirring for 30 minutes and centrifuged for 20 minutes at 6,000 RPM, and an aliquot of the liquid remnant was taken to obtain the UV-Vis spectrum. Figure 6 shows the UV-Vis spectra obtained after adsorption.

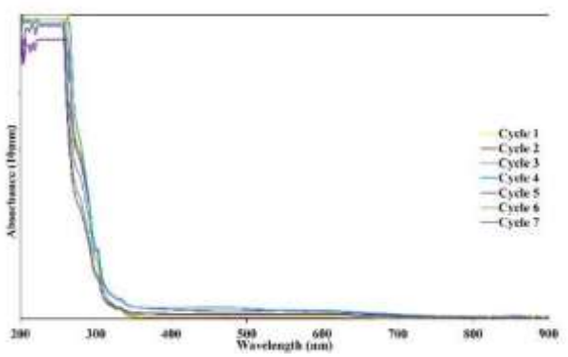

Figure 6 UV-Vis spectrum for the adsorption cycles of AD56 with Er_2BDC_3

In Figure 7, it can be seen that for this material, adsorption between 88 and 99% was obtained; this is because the dye has a small molecular size, as shown in Figure 8. This allows the MOF not to become saturated quickly, resulting in several adsorption cycles.

ISSN: 2410-3934

The maximum adsorption capacity that was obtained with all the cycles was 33.97 mg/g, which, compared to MIL-56 (Cr or Al), exceeds the capacity reported for the methylene blue, which is 20 mg/g (Mohammadnejad *et al.*, 2018). It should be noted that methylene blue is a cationic dye with three benzene rings and sulfur and nitrogen atoms that act as Lewis bases, while disperse blue 56 has N and O.

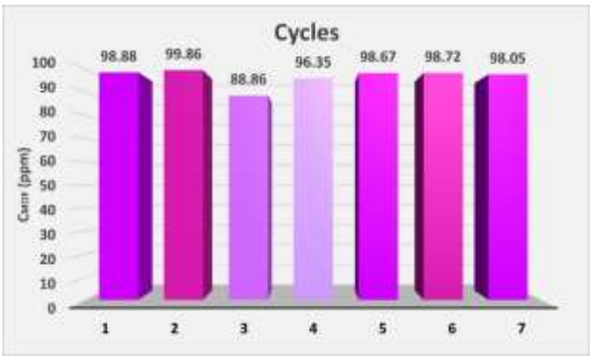

Figure 7 Adsorption histogram for the dye with Er_2BDC_3

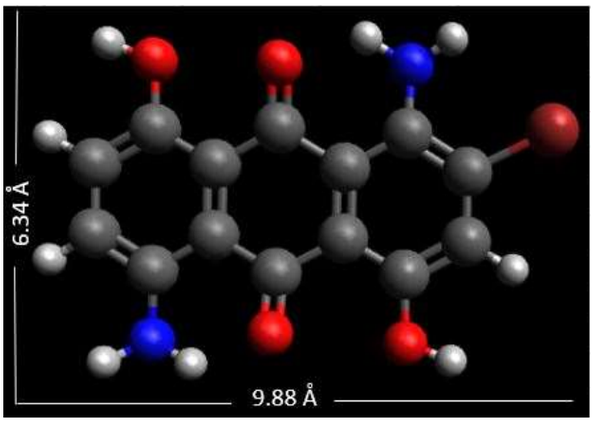

Figure 8 Molecular structure of disperse blue dye 56

Post-adsorption MOF stability

In Figure 1, the diffraction pattern for pristine Er_2BDC_3 presents characteristic peaks to the diffractograms theoretically reported for terbium and erbium. Once the adsorption was carried out, it is observed in the diffractogram of Figure 9, the crystalline structure of the material changed, presenting peaks in the same Bragg angle positions as the simulated diffractogram reported for Tb_2BDC_3 (Reineke *et al.,1999)*, that is to say, that the adsorption for the AD56 dye in the initial structure works as a structural purification process (recrystallization) where the Er_2BDC_3 phase is eliminated and only the Tb_2BDC_3 structure is formed.

This result indicates that it is possible to use the dyes to obtain the purer structure of MOF and that dye molecules present in contaminated water can be eliminated.

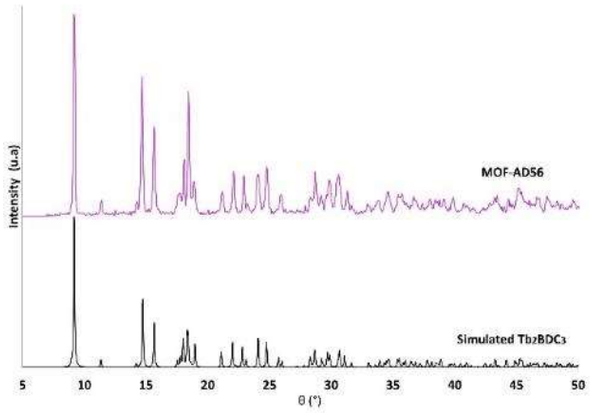

Figure 9 Comparison of the simulated diffractogram of Tb_2BDC_3 and the diffractogram of the MOF with dye AD56 after adsorption

The Debye-Scherrer equation was used to determine the crystal size of the MOF after dye adsorption. The maximum peak of the sample was taken at 9.19° (2θ), and the crystal size D obtained was 44.77 nm. When comparing this crystal size and the data obtained for the structure of Tb_2BDC_3 present in the pristine MOF (table 1), it can be observed that there is a decrease in size. Despite the different Van der Waals interactions by the functional groups present in the dye, crystal aggregation in the MOF is not favored, and there is a noticeable change in crystal size.

Functional groups

Figure 10 represents the FT-IR of Er2BDC3 before and after the adsorption. According to the analysis carried out in *functional groups, from the section on physicochemical properties of the MOF*, it can be seen that there was a variation in the material. At 1159 cm^{-1}, a characteristic band of DMF is observed, which still indicates its presence in the material. It is important to mention that there is a 1,4-disubstituted mononuclear ring in the structure of the dye, corresponding to anthraquinone and in MOF-Er to the presence of BDC, used as an organic ligand. Because of this, two bands are at the same wavelength for both materials. At 752 cm^{-1}, a band is observed by bending =C-H of aromatic rings.

ISSN: 2410-3934

Fernández G. reports that *para*-substituted aromatic rings have two combination bans in a range of 1670-2000 cm^{-1}, but the data obtained experimentally it is observed that these bands are found at 1508 and 1574 cm^{-1}. Finally, for the FT-IR of the MOF with dye after the adsorption, at 886 cm^{-1}, two low-intensity bands belong to the disubstituted aromatic ring, and at 1590 cm^{-1}, there is a low-intensity band corresponding to the bending of the C-H bond of the aromatic ring of anthraquinone, the main compound of the dye.

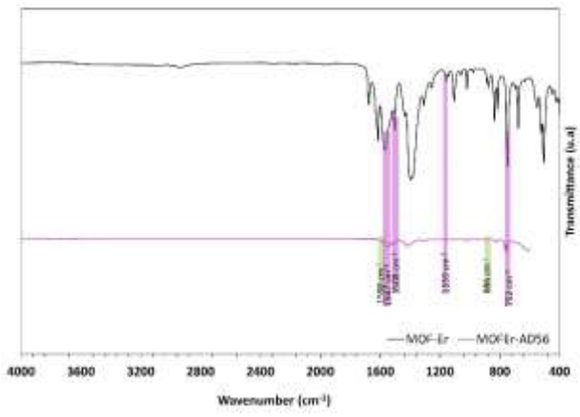

Figure 10 Comparison of FT-IR spectrum of Er_2BDC_3 before and after the adsorption of disperse blue dye 56

Acknowledgment

To the Universidad Autónoma Metropolitana, Unidad Azcapotzalco, for the facilities for this work.

Financing

This work has been funded by CONAHCYT [proyect CB A-S1-31186, 2018].

Conclusions

In this work, microwave synthesis of Er_2BDC_3 was performed and used to remove dye AD56. The MOF was characterized before and after the adsorption of the anthraquinone dye. The result obtained in XDR shows a change in the crystalline structure after adsorption, obtaining a purer material with a single crystalline phase. Also, a change in the crystal size was observed due to the different Van der Waals interactions generated by the functional groups present in the dye. The morphology shows that Er_2BDC_3 presents microstructures of different asymmetric shapes with aggregates from 0.30-1.5 μm.

Also, it is observed that his material has a very porous surface, allowing it to be reused for several cycles to remove dyes. When comparing, the FT-IR is observed that after the removal of the anthraquinone material, two characteristic bands belong to the anthraquinone, which confirms the presence of AD56 in the Er_2BDC_3. Finally, the seven cycles performed obtained a total maximum adsorption capacity of 33.97 mg/g. The degree of adsorption of dyes in Er_2BDC_3 depends on the size of the molecule. The steric effect was notably observed for the AD56 dye, since presenting a small molecule made it possible to adsorb in a higher percentage during the seven cycles. This material is a viable option in wastewater treatment for removing chemical contaminants, particularly dye.

References

Chen, B., Yang, Y., Zapata, F., Qian, G., Luo, Y., Zhang, J., & Lobkovsky, E. B. (2006). Enhanced near-infrared− luminescence in an erbium tetrafluoroterephthalate framework. Inorganic chemistry, 45(22), 8882-8886. https://pubs.acs.org/doi/abs/10.1021/ic060568u DOI: https://doi.org/10.1021/ic060568u

Doval-Leira, R. (2014). Utilización de lodos rojos para la eliminación de contaminantes en efluentes de la industria textil. Recuperado de: https://ruc.udc.es/dspace/handle/2183/13979.

Fernández G. (S.F). Espectroscopia de infrarrojo. Espectro IR: Aromáticos. https://www.quimicaorganica.org/espectroscopia-infrarroja/781- espectro-infrarrojo-de-benceno-y-aromaticos.html?tmpl=component&print=1.

Kennard O. (1965). The Cambridge Crystallographic Data Centre (CCDC), UK. https://www.ccdc.cam.ac.uk/.

Larkin, P.J. (2018). IR and Raman Spectra-Structure Correlations. Infrared and Raman Spectroscopy, Second Edition. https://www.sciencedirect.com/book/9780128041628/infrared-and-raman-spectroscopy DOI: https://doi.org/10.1016/C2015-0-00806-1.

Liu, K., You, H., Zheng, Y., Jia, G., Zhang, L., Huang, Y., ... & Zhang, H. (2009). Facile shape-controlled synthesis of luminescent europium benzene-1, 3, 5- tricarboxylate architectures at room temperature. CrystEngComm, 11(12), 2622- 2628. https://www.researchgate.net/publication/274720543_Facile_shape-controlled_synthesis_of_luminescent_europium_benzene-135-tricarboxylate_architectures_at_room_temperature. DOI: http://dx.doi.org/10.1039/b905924p

Loera-Serna, S., Flores, J., Navarrete-López, A. M., Díaz de León, J. N., & Beltran, H. I. (2019). Composites of Anthraquinone Dyes@ HKUST-1 with Tunable Microstructuring: Experimental and Theoretical Interaction Studies. Chemistry–A European Journal, 25(17), 4398-4411. https://chemistry-europe.onlinelibrary.wiley.com/doi/abs/10.1002/chem.201805548 DOI: https://doi.org/10.1002/chem.201805548

Loera-Serna S., Oliver-Tplentino M. A., López-Núñez Ma. de L., Santana-Cruz A., Guzmán-Vargas A., Cabrera-Sierra R., Beltrán H. I., Flores j., (2012). Electrochemical behavior of [Cu3(BTC)2] metal–organic framework: The effect of the method of synthesis, Journal of Alloys and Compounds, Volume 540, 2012, Pages 113-120. ISSN; 0925-8388. DOI: https://doi.org/10.1016/j.jallcom.2012.06.030. https://www.sciencedirect.com/science/article/pii/S0925838812009991

Martínez, A. C., Olivares, C. C., Lozada, A. E., & Ramírez, C. G. (2014). Contaminación generada por colorantes de la industria textil. Vida Científica Boletín Científico de la Escuela Preparatoria No. 4, 2(3). https://repository.uaeh.edu.mx/revistas/index.php/prepa4/article/view/1862. eISSN: 2007-4905

Mohammadnejad, M., Hajiashrafi, T., & Rashnavadi, R. (2018). An erbium–organic framework as an adsorbent for the fast and selective adsorption of methylene blue from aqueous solutions. Journal of Porous Materials, 25(3), 761-769. https://link.springer.com/article/10.1007/s10934-017-0489-8. DOI: https://doi.org/10.1007/s10934-017-0489-8

Núñez-Bautista, S. S., & Victoria-Rueda, T. J. (2020). Tratamiento de agua residual de la industria textil utilizando nanopartículas magnéticas@ biomasa residual como tratamiento terciario. https://repository.ucatolica.edu.co/server/api/core/bitstreams/7cd6e0cc-3cc4-493b-aa2f-301297fa78a7/content

Piñon Niño, O. O. (2019). Síntesis de un nuevo armazón organometálico de zinc con potencial aplicación en la adsorción de colorantes y producción de carbón por el método de pantilla suave. Tesis de maestría, Universidad Autónoma de Nuevo León. Recuperado de: http://eprints.uanl.mx/18518/.

Reineke, T. M., Eddaoudi, M., Fehr, M., Kelley, D., & Yaghi, O. M. (1999). From condensed lanthanide coordination solids to microporous frameworks having accessible metal sites. Journal of the American Chemical Society, 121(8), 1651-1657. https://pubs.acs.org/doi/10.1021/ja983577d. DOI: https://doi.org/10.1021/ja983577d

Saito, T., Yamaji, T., Hayamizu, K., Yanagisawa, M., Yamamoto, O. Spectral Database for Organic Compounds SDBS by National Institute of Advanced Industrial Science and Technology (AIST), Japón. https://sdbs.db.aist.go.jp/sdbs/cgi-bin/cre_index.cgi

Sorribas, S., & Téllez, C. (2016). MOFs: Propiedades y aplicación en separaciones más eficientes. Boletín del Grupo Español del Carbón, (41), 19-22. https://dialnet.unirioja.es/servlet/articulo?codigo=6164949. ISSN: 2172-6094.

Wang, Y., Kretschmer, K., Zhang, J., Mondal, A. K., Guo, X., & Wang, G. (2016). Organic sodium terephthalate@ graphene hybrid anode materials for sodium-ion batteries. RSC advances, 6(62), 57098-57102. https://pubs.rsc.org/en/content/articlelanding/2016/RA/C6RA11809G. DOI: https://doi.org/10.1039/C6RA11809G